

Central Lancashire Online Knowledge (CLoK)

Title	Evaluating polyanthranilic acid as a polymeric template for the production of Prussian blue nanoclusters
Type	Article
URL	https://clok.uclan.ac.uk/id/eprint/52484/
DOI	https://doi.org/10.1007/s10853-024-10023-w
Date	2024
Citation	Gilpin, Victoria, McCormick, Rachel, McMath, Regan, Smith, Robert B, Papakonstantinou, Pagona and Davis, James (2024) Evaluating polyanthranilic acid as a polymeric template for the production of Prussian blue nanoclusters. Journal of Materials Science, 59. pp. 14245-14258. ISSN 0022-2461
Creators	Gilpin, Victoria, McCormick, Rachel, McMath, Regan, Smith, Robert B, Papakonstantinou, Pagona and Davis, James

It is advisable to refer to the publisher's version if you intend to cite from the work. https://doi.org/10.1007/s10853-024-10023-w

For information about Research at UCLan please go to http://www.uclan.ac.uk/research/

All outputs in CLoK are protected by Intellectual Property Rights law, including Copyright law. Copyright, IPR and Moral Rights for the works on this site are retained by the individual authors and/or other copyright owners. Terms and conditions for use of this material are defined in the http://clok.uclan.ac.uk/policies/

Chemical routes to materials



Evaluating polyanthranilic acid as a polymeric template for the production of Prussian blue nanoclusters

Victoria Gilpin¹, Rachel McCormick¹, Regan McMath¹, Robert B. Smith², Pagona Papakonstantinou¹, and James Davis^{1,*}

Received: 24 April 2024 Accepted: 13 July 2024

© The Author(s), 2024

ABSTRACT

The electropolymerization of anthranilic acid (2-aminobenzoic acid) has been shown to lead to the production of a redox polymer functionalized with carboxylate groups capable of complexing metal ions. The polymer was exploited as a means of capturing ferric ion from solution with the iron decorated polymer chains used as seeding points for the formation of Prussian blue (PB). Nanoclusters of PB were dispersed throughout the three-dimensional polymer matrix with deposition achieved through direct electrochemical means or via a dip process. The latter exploited the chemical combination of Fe(III) + Ferrocyanide to yield PB allowing its dispersal of the PB throughout the polymer film. The polymer film and its subsequent modification have been characterized by electron microscopy, X-ray analysis, Raman spectroscopy and electrochemical analysis. The stability toward peroxide has also been explored.

Handling Editor: Dale Huber.

Address correspondence to E-mail: james.davis@ulster.ac.uk

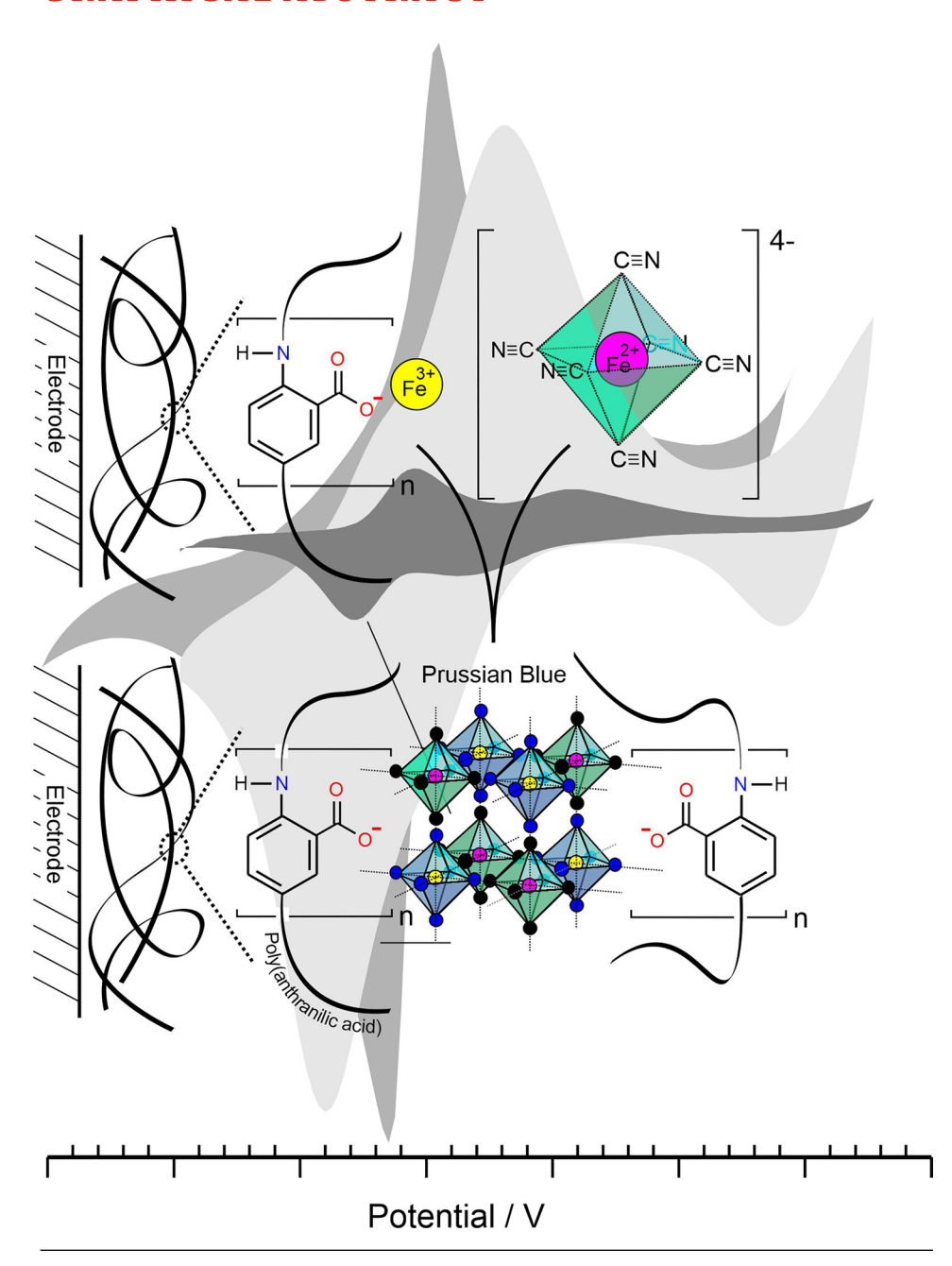
Published online: 30 July 2024



¹ School of Engineering, Ulster University, Belfast, Northern Ireland BT15 1ED, UK

² School of Engineering and Computing, University of Central Lancashire, England Preston, PR1 2HE, UK

GRAPHICAL ABSTRACT



Introduction

The versatility of Prussian blue (PB) as an electroresponsive material is well established and through its various forms (film or particle), it has found use in a large spectrum of applications that include: electrochromic devices, solid-state batteries and sensors [1–3]. Its electrocatalytic properties, however, have long formed the basis of biosensor systems where it has proven to be particularly adept at enhancing the detection of peroxide resulting from oxidase enzyme-type reactions [4–7]. Its inorganic origin has often led to it being described as an artificial peroxidase or nanozyme [8–11] facilitating



the electroreduction of peroxide at low potentials (typically around 0.V vs Ag|AgCl). In doing so, the current contribution from common interferences (ascorbate, urate, etc.) is avoided or greatly reduced [12–16]. The production of nanostructured PB in particular has garnered considerable interest where the production of PB nanoparticles has been shown to exhibit catalytic constants some 4 orders of magnitude higher than those observed with natural peroxidases [17, 18]. The superior performance of nanoparticle/nanocluster PB toward peroxide reduction over conventional polycrystalline film has also been reported and has been attributed to PB with small size, large surface-to-volume ratio and increased surface activity [19–21]. While PB can be produced by chemical or electrochemical means, the latter offers a simple method which provides a high degree of control over the PB formation and deposition process. Spatial and morphological control can often be achieved ranging from nanoparticles/cluster (nanozyme) systems to extensive films such that the catalyst can be incorporated into a variety of sensing formats.

Despite the many features of PB, it can often exhibit stability issues where leaching of the catalyst to the solution occurs, thereby compromising the performance and lifetime of the sensor [22, 23]. This is especially problematic in solutions of neutral or alkaline pH. One approach to addressing such limitations has involved the use of protective membranes as a means of entrapping the PB and reducing its ability to diffuse away. These have included preformed polymers such as Nafion®[24-26] and chitosan [27–29]. Unfortunately, issues of uniformity in coverage, swelling, compatibility with other biocomponents that form the sensor and the influence on reproducibility can limit their applicability. Conducting polymers have been proposed as an alternative to the conventional membrane systems where electrochemical deposition can offer far greater control over the PB fabrication method [30-34]. However, it also enables the particular chemical and electronic properties of the polymer to be directly harnessed and integrated with the nano-PB structures. Polyaniline (PANI) is arguably of the most well recognized of the conducting polymers and known to possess high conductivity while offering a high degree of control over film formation and homogeneity [35–38]. It is perhaps little surprise that PANI/PB composites have been studied and used as a matrix for sensors [31–38]. However, once the solution pH is increased beyond pH 4, PANI loses its electrochemical activity [38–40]. This has prompted a search for alternative PANI systems in order to widen the pH range within which the polymer activity is retained.

It is known that in PANI, the electroactivity of the polymer backbone is maintained only in solutions of low pH where there is a high degree of protonation at the imine nitrogen atoms [38, 39]. It has been previously postulated that the incorporation of acidic functional groups into the polymer backbone could therefore alter the micro-environment of the imine centers, thereby influencing the local pH and thereby facilitating redox activity [39, 40]. This has been supported by experiment where polymerization of aniline derivatives bearing carboxylic acid [39-45], phosphonic acid [46] or sulfonic acid [47, 48] substituents has led to films that retain electroactivity in solutions whose pH is neutral or moderately alkaline. However, these functional groups also impart additional chemical properties that can allow the films to be tailored. One aspect is that acid groups result in a "self-doped" systems which modify the ion exchange properties of the film. The anionic groups counterbalance the positive charge generated along the oxidized PANI backbone. In contrast to conventional homopolymer PANI, electrolyte anions are not exchanged during redox cycling [39–45].

A second aspect, which is more pertinent to the present investigation, is the ability of aniline-carboxylic acid functionalities to coordinate metal ions [41–46]. Considering a polymer composed of repeating 2-aminobenzoic acid units joined head to tail to form polyanthranilic acid (PAA). The backbone could be expected to possess the key attributes of PANI, while the COOH group acts as capture points for ferric ion with the chain length being effectively decorated with the metal ion as indicated in Fig. 1A.

It could be envisaged that upon exposure of the PAA-Fe(III) film to ferrocyanide, PB formation should occur should resulting in the generation of catalytic PB clusters throughout the film as indicated in Fig. 1B. It was anticipated that the nanoclusters would provide an enhanced response to peroxide with the "self-doped" nature of the PAA serving as molecular wire to the underlying electrode. In this instance, carbon fiber was chosen as the substrate providing a highly conductive base through which to characterize the proposed composite. While PAA has been used to template the production of iron oxide nanoparticles [35, 43], this



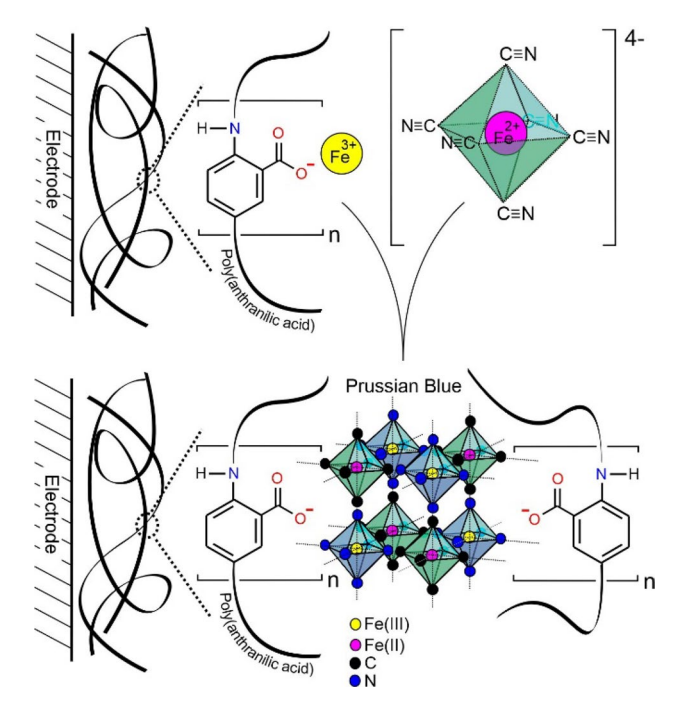


Figure 1 A Coordination of ferric ion at a polyanthranilic acid modified electrode and **B** where exposure to ferrocyanide leads to the formation of Prussian blue clusters.

is the first report of PAA being used in combination with PB. As such, the aims of the investigation were to characterize the formation of PAA film on carbon fiber, assess its applicability to template the formation of PB and critically evaluate the performance of the composite structure toward the reduction of peroxide.

Experimental details

All reagents were of the highest grade available and were obtained from Sigma and used without further purification. Solutions of ferric chloride, ferricyanide and ferrocyanide were prepared daily. Toray carbon fiber (TGP-H-60, 19 × 19 cm) was used as the electrode substrate throughout and was purchased from Alfa Aesar (Thermo Fisher Scientific, UK). Electrochemical analysis was conducted at 22 °C ± 2 °C using a Zimmer Peacock Anapot potentiostat running PSTrace software (Version 5.9). Initial investigations employed a standard three-electrode configuration where either a carbon fiber sheet or glassy carbon (3 mm diameter, BAS Technicol) served as the working electrode. Platinum wire served as the counter electrode and a commercial Ag | AgCl half cell (3 M NaCl) as the reference. The carbon fiber electrode was prepared through thermally encapsulating a portion of the fiber mat (5 mm × 5 mm) into polyester laminates that had been precut with a 3 mm × 3 mm square window (Figures S1 and S2). This was to expose the carbon fiber surface and served to control the geometric area of the working electrode in a manner similar to that reported by Casimero et al. [49]. In general, the carbon fiber electrode subsequently modified through electrochemical anodization (+1.5 V, 300 s, 0.1 M NaOH). Raman spectra of the PAA-PB samples were obtained using a Renishaw Raman Microscope (20 × objective lens) with a 45 -W, 532-nm laser operating at 10% power. Scanning electron microscopy (SEM) was performed with a Hitachi SU5000 FE-SEM equipped with an Oxford Instruments Energy-Dispersive X-Ray Analysis (EDX) system. This allowed investigation of the surface characteristics of the electrodes during the various stages of modification and to map the elemental distribution—particularly the spread of PB clusters.

Preparation of Prussian blue films

The electrochemical preparation of PB was conducted using a process similar to that detailed by Barber et al. (2023) and involved the use of repetitive scan cyclic voltammetry [27]. A carbon fiber (or glassy carbon) electrode was employed as the working electrode and placed in a solution containing 2 mM ferric chloride, 2 mM potassium ferricyanide, 0.1 M KCl and 0.1 M HCl. The latter was used to maintain an acidic matrix [27]. The potential range + 0.8 V to -0.4 V was scanned at 50 mV/s resulting in the layer by layer deposition of PB. A chemical approach to the formation of PB was pursued in the later stages where the in situ reaction of ferric ion coordinated within the polyanthranilic acid film with ferrocyanide was expected to lead to the direct formation of PB. In this case, a carbon fiber electrode coated with polyanthranilic acid was dipped into 2 mM Ferric nitrate for periods up to 12 h and rinsed with copious amount of water to remove unbound ferric ion. The electrode dipped into 2 mM ferrocyanide to induce the formation of PB and then rinsed with deionized water prior to use.

Results and discussion

Prussian blue deposition on carbon fiber

Cyclic voltammograms detailing the response of the carbon fiber (CF) electrode toward ferrocyanide



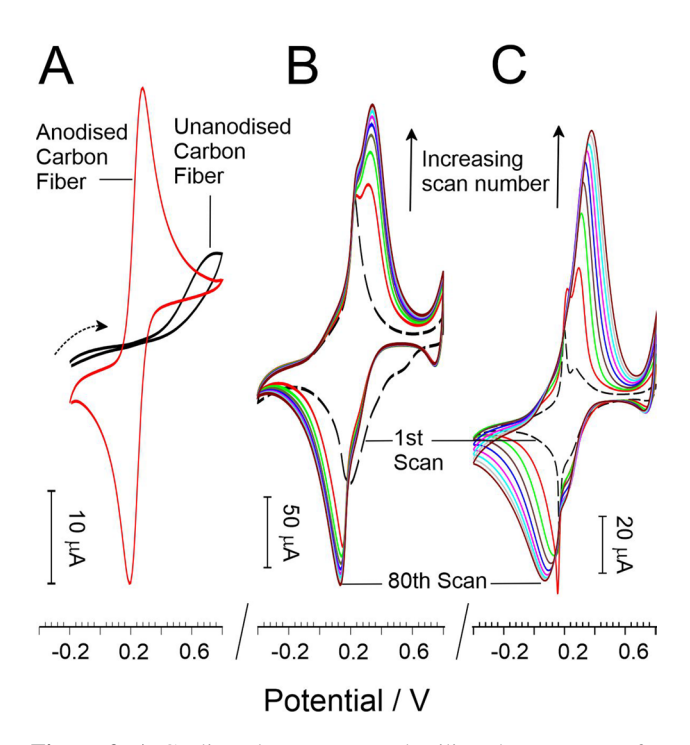


Figure 2 A Cyclic voltammograms detailing the response of a carbon fiber electrode (CF) toward ferrocyanide (2 mM in 0.1 M KCl, 50 mV/s) before and after anodization. (B,C) Cyclic voltammograms detailing the response of a CF. **B** electrode and a glassy carbon. **C** Electrode in a solution containing 2 mM ferric chloride and 2 mM ferricyanide (0.1 M HCl, 50 mV/s) resulting in the cumulative deposition of Prussian blue.

before and after anodization of the fiber surfaces are compared in Fig. 2A. Pre-anodization, the response is very poor with a very large over potential required to induce electron transfer. In contrast, the anodized fiber provides a cyclic voltammetric profile that is near reversible with a peak separation of 80 mV. This disparity can be attributed to basal plane nature of the unmodified carbon structure with anodization resulting in exfoliation and the production of edge planes. Moreover, the anodization process is known to result in greater oxygen functionality which facilitates fast electron transfer to ferrocyanide [49]. As such, anodized CF electrodes were adopted for the subsequent investigations. The electrochemical formation of Prussian blue at an anodized CF electrode is detailed in Fig. 2B, and it can be seen that the magnitude of the redox peaks increases with each scan as the PB is formed. The deposition of the PB onto the CF electrode is compared with a similar process using a glassy carbon electrode (Fig. 2C). It can be seen that same redox processes occur and are similar to those reported with laser-induced graphene substrates [27].

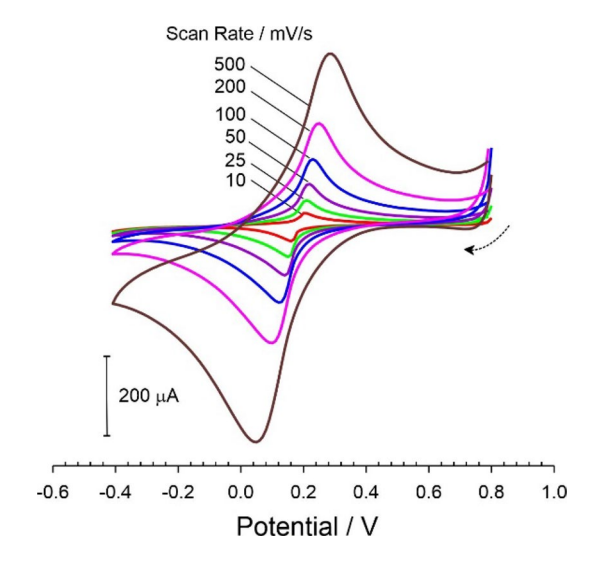


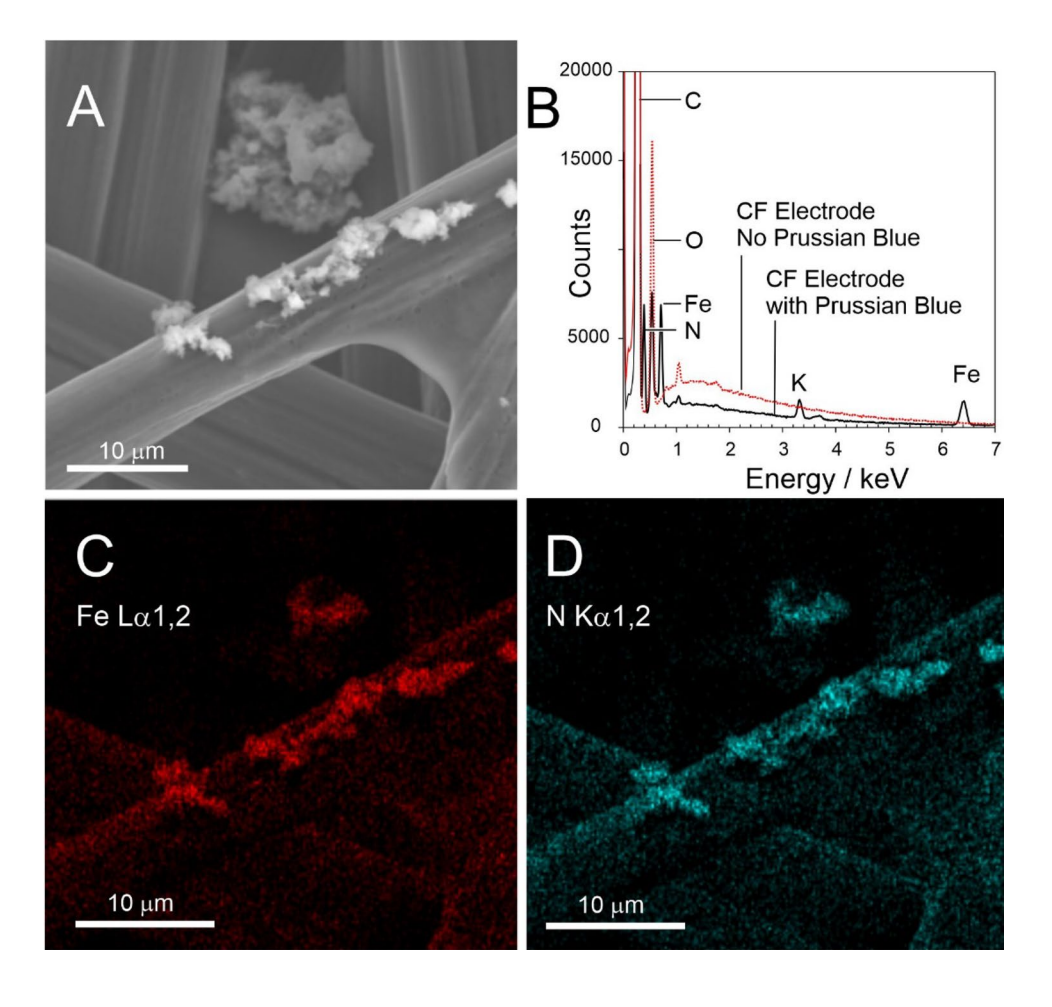
Figure 3 Cyclic voltammograms detailing the response of a Prussian blue modified carbon fiber (CF) electrode in 0.1 M HCl at various scan rates.

The PB voltammetric profile was retained when cycled in fresh 0.1 M HCl as indicated in Fig. 3 with the Randles-Sevcik relationship between peak height (Ip) and the square root of scan rate (v^{1/2}), Figure S3, exhibiting a linear trend (where $Ip_{(anodic)}$ (/µA) = 682.2 $\nu^{1/2}$ (V/s) -53; R^2 = 0.999; $Ip_{(cathodic)}$ (/µA) = -830.4 $\nu^{1/2}$ (V/s) + 63.9; R^2 = 0.995; N = 6). This runs counter to the normal expectation for a surface-confined species and implies that the current response is diffusion limited. Nevertheless, the response is consistent with previous reports of PB deposited onto various carbon substrates [27, 50] and could be attributed to the requirement for the insertion of a counter ion (i.e., K^+) into the crystal structure during redox cycling [50].

Corroboration for the immobilization of PB on the electrode surface was achieved through SEM–EDX analysis and surface mapping of Fe distribution. At first glance, the initial deposition of PB appears as sporadic PB crystal clusters located on the CF framework (Fig. 4A). EDX analysis was used to confirm the presence of Prussian blue on the coated electrode (Fig. 4B). EDX mapping, highlighted in Fig. 4C, D, confirms a high density of Fe/N at the microclusters, but, critically, it can be seen that there is a uniform distribution of Fe/N across the CF surface. These discrete Fe/N elemental signatures can be attributed to nanoparticulate PB which has initially nucleated at defect sites across the CF surface. Further elemental



Figure 4 A Scanning electron micrograph of a Prussian blue-coated CF framework. B EDX spectra comparing CF electrodes with and without Prussian blue deposits. (C,D) EDX mapping of Fe and N distribution across the CF network.



analysis of a coated CF-PB electrode reveals atomic %wt contribution of 11.9% and 7.9% for Fe and N, respectively. This gives rise to a N: Fe atomic ratio of 2.66 which is in close agreement with the theoretical ratio of 2.57 associated with conventional Prussian blue formula of $Fe_4[Fe(CN)_6]_3$. It is important to note that there is no nitrogen nor iron EDX signature from the unmodified or anodized carbon fiber samples themselves (Fig. 4B).

It is known that the anodization process will increase the population of defect sites at the CF interface [49] and it could be anticipated that these are a key contributor to the disperse formation of nano-PB. In addition, the anodic generation of carboxylic acid groups during the pretreatment phase could be expected to initially coordinate the Fe (III) and thereby assist the nucleation process in much the same way as the proposed methodology outlined in Fig. 1. However, it must be noted that the proliferation of nano-PB clusters at the bare electrode is, at least initially, likely to be 2 dimensional. In

contrast, it was envisaged that the proposed use of polyanthranilic acid, with an abundance of COOH functional groups throughout the polymer backbone, could allow the generation of a 3-dimensional network of similarly nano-sized PB clusters.

Polymerization of anthranilic acid

Cyclic voltammograms detailing the electropolymerization of anthranilic acid (10 mM, 0.1 M HCl, 50 mV/s) are detailed in Fig. 5A. The initial irreversible oxidation process commences at + 0.9 V with the deposition of a conductive film evidenced by a series of redox peak which increase in magnitude on subsequent cycles. The cyclic voltammetric redox signatures of the PAA modified electrode in fresh 0.1 M HCl at various scan rates are highlighted in Fig. 5B. The relationship between peak height (Ip) and scan rate, Figure S4, was found to be linear (where $Ip_{(anodic)}$ (/ μ A) = 268.6 ν (V/s) + 3.85; R^2 = 0.992; $Ip_{(cathodic)}$ (/ μ A) = -263.5 ν



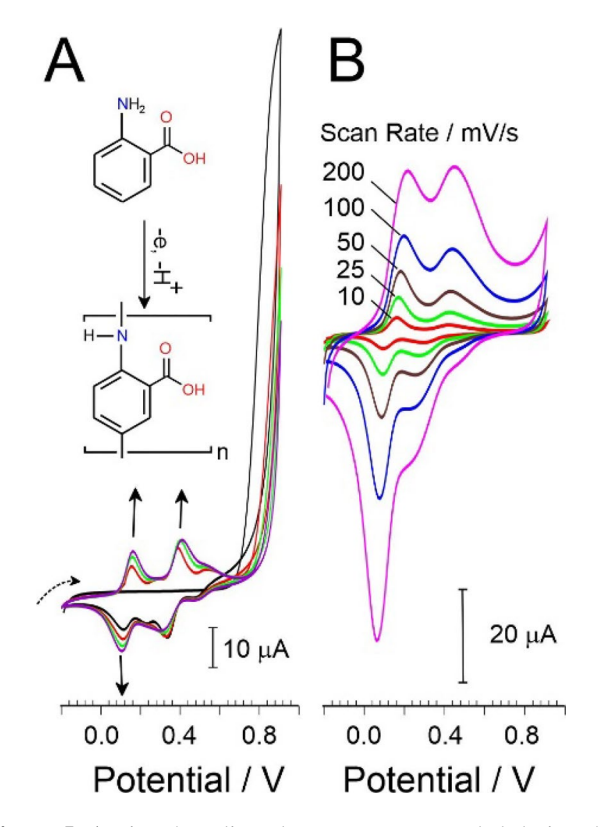


Figure 5 A First 4 cyclic voltammograms recorded during the electropolymerization of anthranilic acid (10 mM, 0.1 M HCl, 50 mV/s) at an anodized carbon fiber electrode. **B** Polyanthranilic acid film (after 20 scans) modified carbon fiber electrode at various scan rates in fresh 0.1 M HCl.

(V/s) -4.13; R^2 = 0.997; N = 6) and is consistent with the behavior expected for a surface-confined species.

The redox peaks of the polyanthranilic acid film highlighted in Fig. 5B can be attributed to interconversions analogous to those of polyaniline. These are detailed in Fig. 6 and include (A) leucoemeraldine (fully reduced), (B&C) emeraldine (half oxidized) and (D) pernigraniline (fully oxidized) [35–39]. In contrast to polyaniline, the carboxylate group enables self-doping allowing the film to retain conductivity in solutions of higher pH [38–40].

Polyanthranilic acid—Prussian blue composite

The PAA modified electrode was placed in a solution containing equimolar ferric chloride and ferricyanide (2 mM, 0.1 M KCl). As both iron species are in the highest oxidation state, both coexist without any conversion to Prussian blue. It was anticipated however that the ferric ions would be co-ordinated to the carboxylate functionalities on the PAA-much in the same way as that proposed with the anodized carbon fiber (Fig. 1). Upon cycling the ferricyanide to ferrocyanide, reaction between the Fe(II) and Fe(III) components was expected to occur resulting in the nucleation of Prussian blue clusters. Cyclic voltammograms detailing the response of the PAA modified electrode in the Fe (III) ion/ferricyanide solution are detailed in Fig. 7A. Well-defined redox peaks characteristic of PB were observed and found to increase in magnitude with increasing scan number. The voltammetric profiles observed at the CF electrode after the various stages of modification are compared in Fig. 7B. It can

Figure 6 Redox transitions of a polyanthranilic acid homopolymer. **A** Leucoemeraldine, **B-C** emeraldine base and salt. **D** Pernigraniline (adapted from [39]).

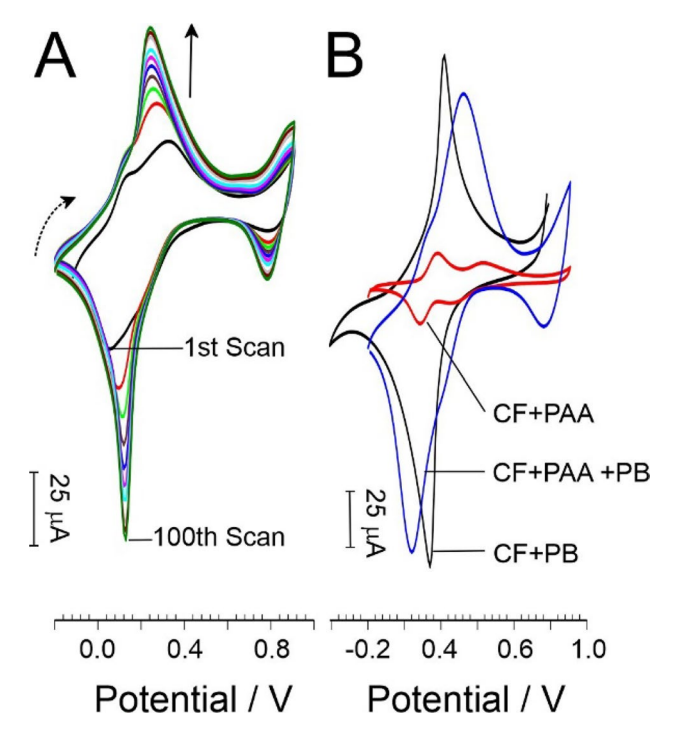


Figure 7 A Cyclic voltammograms detailing the response of a polyanthranilic acid (PAA) modified carbon fiber (CF) electrode in a solution containing equimolar Fe(III)/ferricyanide (2 mM, 0.1 M KCl, 50 mV/s) resulting in the production of Prussian blue (PB). **B** Voltammograms comparing the response of the carbon fiber electrode at various stages of modification in fresh 0.1 M HCl. Scan rate in all cases: 50 mV/s.

be seen that the PB redox profiles within the PAA are broader than those observed with the simple CF-PB electrode, but, critically, the position of the PAA-PB reduction peak has been shifted cathodically by 100 mV to + 0.04 V. This could be significant in terms of the catalytic reduction process where the detection potential associated with the reduction peak needs to be as low as possible in order to avoid interference from other electroactive components that may be in the sample.

Scanning electron microscopy of the PAA modified fibers revealed that the fibers were uniformly coated (Fig. 8A) though visible microdefects in structure were observed. Closer inspection of a defect site where the underlying CF is exposed (Fig. 8B) confirms a dense, thin film.

The presence of PB was again confirmed through EDX analysis and by Raman spectroscopy. Representative spectra profiling the CF before and after the sequential electrodeposition of PAA and PB are detailed in Fig. 9. The characteristic D, G and 2D peaks

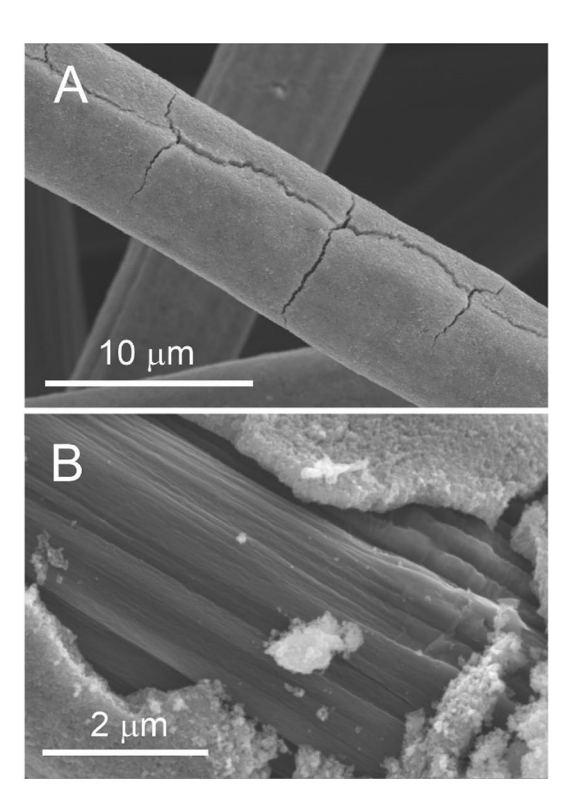


Figure 8 A Scanning electron micrographs of polyanthranilic acid—Prussian blue (PAA-PB) modified fibers. **B** Closer inspection of a defect site highlighting the underlying carbon fiber rod encased in fractured PAA-PB film.

associated with the underlying carbon can be observed at 1354, 1580 and 2716 cm⁻¹, respectively [49, 51, 52]. The D band is typically regarded as being representative of a disordered graphitic structure and arises from the stretching of the sp³ carbons at the terminating edges of the graphene sheets [53, 54]. For the unmodified fiber, the ratio of the intensities associated with the D and G peaks (I_D/I_G) was found to be 0.28 and is relatively low, suggesting that the unmodified bulk is largely basal plane with few defects. This would contrast the observations of electrode structures comprised of graphenic materials (i.e., laser-induced graphene electrodes) where similar Raman analysis revealed an I_D/I_G ratio of 0.79 [27]. Casimero et al. (2019) demonstrated that the I_D/I_C ratio could be easily manipulated through prolonged anodization (25 min) of the carbon fiber [49]. This was found to lead to substantial exfoliation of the carbon ($I_D/I_G = 1.41$), but this led to significant deterioration of the fibers. Significantly, the presence of PB within the film was confirmed by the characteristic peaks at 274, 527, 2098 and 2153 cm⁻¹ [55] and was consistent with previous



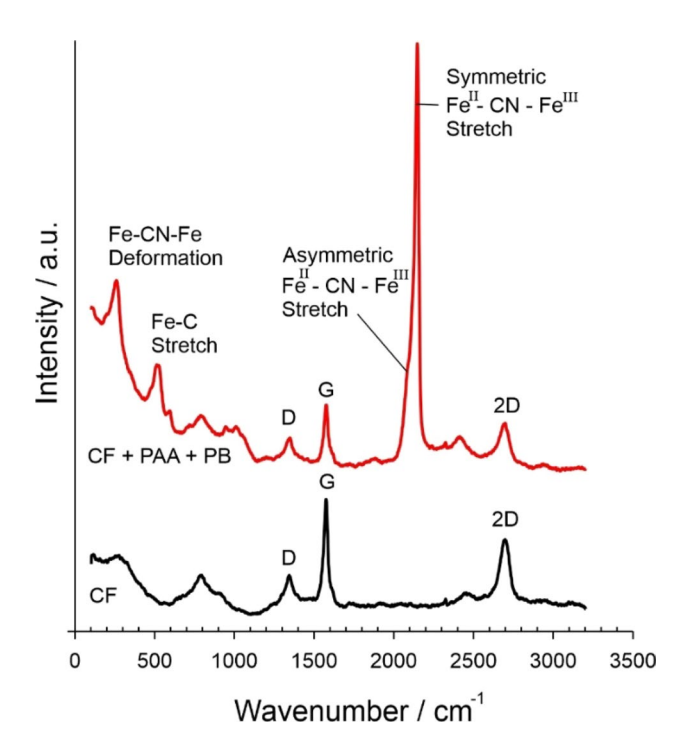


Figure 9 Raman spectra comparing the polyanthranilic acid (PAA) Prussian blue (PB) film with an unmodified carbon fiber (CF) electrode, where the PB was electrodeposition through the PAA film by cyclic voltammetry.

reports of PB electrodeposited onto carbon surfaces [12, 27]. Their respective assignments are highlighted in Fig. 9.

The primary bands at 2098 and 2146 cm⁻¹ are attributed to the asymmetric and symmetric stretch vibrations of $Fe^{II} - C = N - Fe^{III}$, respectively, and provide a clear indication as to the presence of the PB [57-60]. The frequency of the cyanide vibration stretching mode, v(CN), is known to be sensitive to the oxidation state of the coordinating iron such that v(CN) coordinated to Fe(III) displays higher wavenumber peaks than that coordinated to Fe(II) [58, 59]. Two Raman peaks can be observed at 2098 and 2146 cm⁻¹ (albeit the former is more of a shoulder) and confirm the coexistence of Fe(II) and Fe(III). It is worthwhile emphasizing that PB was formed by repetitive cycling in acid conditions (0.01 M HCl with 0.1 M KCl) and thus ensured that no hydroxide ions were present within the coordination spheres of the ferrous center [22]. It should also be noted annealing at 100 °C did not yield any change in the film structure nor the subsequent electrochemical behavior.

Polyanthranilic acid—templating process

Thus far, the PAA coating has served as a three-dimensional matrix through which the PB was electrodeposited. However, it was originally postulated that the carboxyl functionalities could coordinate the ferric ion and thus PB nanoclusters could be formed chemically through simply inserting the PAA-Fe(III) electrode into the a solution of ferrocyanide. It could be anticipated that the three-dimensional material provided by the PAA would therefore yield a film comprised on discrete PB clusters. The approach was therefore investigated through first immersing the PAA modified CF electrode into a ferric nitrate solution (2 mM) for 12 h. The electrode was then removed, rinsed with copious amounts of deionized water and then immersed in a solution containing ferrocvanide (2 mM, 0.1 M KCl) for up to 12 h. The electrode was removed, thoroughly rinsed and cyclic voltammograms recorded in acid solution (0.01 M HCl, 0.1 M KCl, 50 mV/s). The voltammetric sweeps of the PAA and PAA-dipped PB electrode are compared in Fig. 10A. The Prussian blue redox oxidation and reduction processes were observed at + 0.235 V and + 0.162 V, respectively. The presence of the PB confirmed through Raman spectroscopy (Fig. 10B) where the characteristic Fe-CN-FE stretch vibrations were again observed (cf. Figure 9).

The instability of PB immobilized on electrodes has long been recognized [22], and a decrease in the height of the PB redox peaks was observed with repetitive scanning. A 9% decrease in the peak current magnitude was observed after 30 scans with the dip-template produced electrode. In contrast, the electrodeposited PAA-PB exhibited only a 1% decrease after the same scan number. The difference could be attributed to the smaller quantity of PB and its more diffuse nature within the PAA film leading to slow leaching to the solution bulk. Nevertheless, it is clear that the templating approach postulated in Fig. 1 was indeed viable though the potential yield of PB is markedly smaller.

Response to peroxide

As the electrodeposited PAA-PB system gave more significant redox peaks, this method of fabrication was initially used to provide electrode substrates for the peroxide reduction investigations. The electrocatalytic reaction of PB with peroxide is well known and the reaction processes are highlighted in Eqs. 1 and 2 and



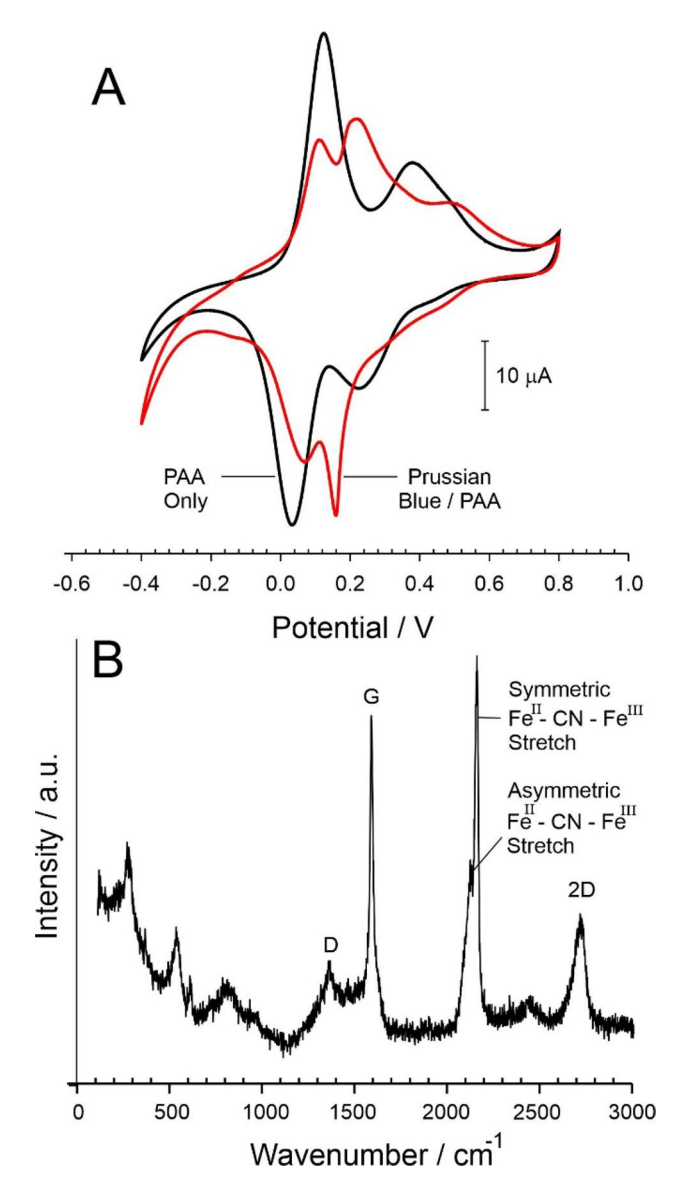


Figure 10 (A) Cyclic voltammetric scans comparing a poly(anthranilic acid) modified carbon fiber electrode before and after modification with Prussian blue via a dip processing technique (0.01 M HCl,0.1 M KCl, 50 mV/s). Inset: Raman spectrum of the electrode confirming the presence of the Prussian blue.

are attributed to the conversion of PB to Prussian white (PW) [22, 23, 60, 61].

$$\begin{split} \operatorname{Fe_4} \big[\operatorname{Fe}(\operatorname{CN})_6 \big]_{3(\operatorname{PB})} &+ 4\mathrm{e} + 4\mathrm{K}^+ \Leftrightarrow \operatorname{Fe_4} \mathrm{K_4} \big[\operatorname{Fe}(\operatorname{CN})_6 \big]_{3(\operatorname{PW})} \\ & (1) \\ \operatorname{Fe_4} \mathrm{K_4} \big[\operatorname{Fe}(\operatorname{CN})_6 \big]_{3(\operatorname{PW})} &+ 2 \operatorname{H_2O_2} \Leftrightarrow \operatorname{Fe_4} \big[\operatorname{Fe}(\operatorname{CN})_6 \big]_{3(\operatorname{PB})} \\ &+ 4 \operatorname{OH}^- &+ 4\mathrm{K}^+ \end{split} \tag{2}$$

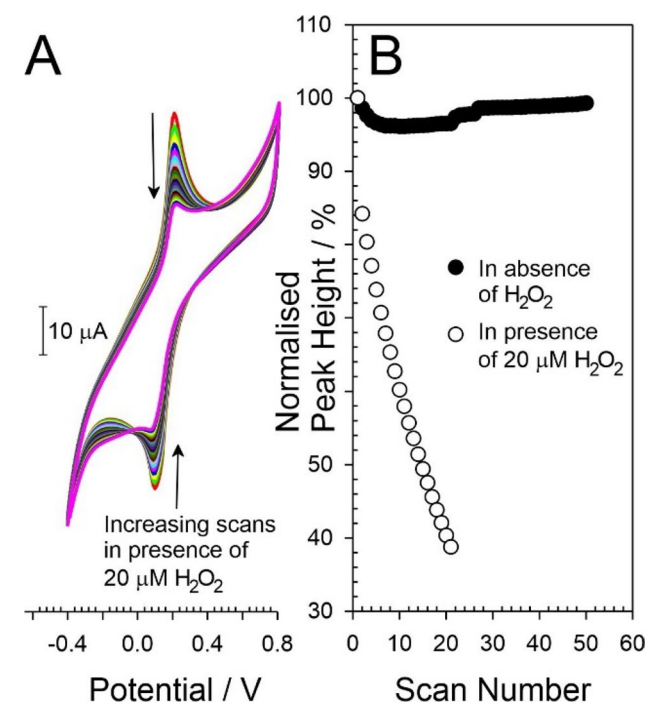


Figure 11 (A) Repetitive scan cyclic voltammograms of a poly(anthranilic acid)-Prussian blue (PAA-PB) polymer in the presence of 20 mM peroxide (pH 7 Britton-Robinson Buffer, 0.1 M KCl, 50 mV/s). (B) Stability comparison of the PAA-PB polymers in the presence and absence of peroxide.

While the electrodeposited PAA-PB electrode was essentially stable to repetitive scanning, it was found to degrade upon the addition of 20 µM peroxide. Cyclic voltammograms detailing the response of the PAA-PB electrode in pH 7 Britton Robinson buffer (with 0.1 M KCl) are shown in Fig. 11A. The initial voltammogram is characteristic of that shown previously in acid solution with the PB reduction peak observed at + 0.05 V. However, upon the addition of peroxide, a decrease in the magnitude of the peak was observed which continued to decrease with each successive scan (Fig. 11B). It would appear that the reaction of the peroxide with the Prussian white form leads to instability of the cluster and its subsequent loss from the polymer matrix. This was also found when cycling the polymer in the acid (0.01 M, 0.1 M KCl).



It has been noted the COOH groups on anthranilic acid impose a steric hinderance during polymerization—increasing interchain distance and leading to a more open structure [62] and, as such, it may be possible that the film may be too porous to provide a sufficient entrapment network. The prevalence of the anionic carboxylate groups could further hinder stability at higher pH, where the network essentially repels the PB clusters. This property of PAA has previously been proposed as a means of reducing the action of negatively charged interferences such as ascorbate and urate [63]. This would be in contrast to those PB systems employing chitosan which have reported increased stability of the PB layer and where the polymer film will be cationic [27, 28]. However, it must be noted that the repetitive electrochemical cycling between PB and PW does not lead to any significant loss redox activity and it is only when there is a chemical interaction between the PW and peroxide that the system becomes unstable and electroactivity is lost.

Nikitina et al. (2023) investigated the templated production of nanoclusters of PB chemically with aniline through a reverse micellar process and were able to transfer the nanoparticles to a glassy carbon electrode [63, 64]. They note that annealing at 100 °C was critical in achieving stability, but similar processing here did not lead to any significant changes in either the surface morphology or electrochemical properties of the PAAsuspended PB and did not improve the stability of the nano-PB in the presence of peroxide. While it would appear that the chemical reaction of the peroxide with PW leads to the dissolution of the nano-PB leading to its subsequent loss, coating the electrode with Nafion did not prevent the loss of redox signature and would again suggest that there is a substantial change in the intrinsic PB structure.

Conclusions

A novel approach to the template formation of Prussian blue nanoclusters using a polyanthranilic acid polymer. The carboxylate functionality of the polymer has been shown to coordinate ferric ion which can be used as seeding points for the subsequent nucleation of PB clusters. The nanoclusters were found to react with peroxide, but rather than the expected

electrocatalytic response, the electrochemical formation of Prussian white and its subsequent reaction with peroxide leads to the dissolution of the cluster structure and loss of activity. This is in marked contrast to the behavior observed with PB film-based structures and could be attributed to the diffuse nature of the clusters within the polymeric framework. This could have significant ramifications when considering polymer seeding as a route to PB nanoparticles. Nevertheless, the ability to template PB has been proven and the polymer provides a simple solution processing strategy for the production of the PB centers.

Acknowledgements

We wish to thank the Department for the Economy, Northern Ireland, for supporting this work

Author contributions

JD, PP, RBS. conceptualized the study; JD. helped in methodology; VG, RMcC, RMcM. contributed to formal analysis and investigation; JD, RBS contributed to writing—original draft preparation; VG, RMcC, RMcM, JD, PP, RBS, PP. helped in writing—review and editing; JD, VG. visualized the study; JD, PP supervised the study, administrated the project and acquired the funding. All authors have read and agreed to the published version of the manuscript.

Data availability

The raw data from relating to electrochemical and spectral characterization are available on request.

Declarations

Conflicts of interest The authors declare no conflicts of interest and the funders had no role in the design of the study; in the collection, analyses or interpretation of data; in the writing of the manuscript; or in the decision to publish the results.



Supplementary Information The online version contains supplementary material available at https://doi.org/10.1007/s10853-024-10023-w.

Open Access This article is licensed under a Creative Commons Attribution 4.0 International License, which permits use, sharing, adaptation, distribution and reproduction in any medium or format, as long as you give appropriate credit to the original author(s) and the source, provide a link to the Creative Commons licence, and indicate if changes were made. The images or other third party material in this article are included in the article's Creative Commons licence, unless indicated otherwise in a credit line to the material. If material is not included in the article's Creative Commons licence and your intended use is not permitted by statutory regulation or exceeds the permitted use, you will need to obtain permission directly from the copyright holder. To view a copy of this licence, visit http://creativecommons.org/licenses/ by/4.0/.

References

- [1] Zhang Y, Li W, Gong H, Zhang Q, Yan L, Wang H (2024) Recent progress in prussian blue electrode for electrochromic devices. Front Energy. https://doi.org/10.1007/ s11708-024-0927-7
- [2] Wang P, Sun S, Bai G, Zhang R, Liang F, Zhang Y (2024) Nanosized Prussian blue and its analogs for bioimaging and cancer theranostics. Acta Biomater 176:77–98
- [3] Kitchamsetti N (2023) A review on recent advances in Prussian blue, its analogues, and their derived materials as electrodes for high performance supercapacitors. J Energy Storage 73:108958
- [4] Karyakin AA (2017) Advances of Prussian Blue and its analogues in (bio)sensors. Curr Opin Electrochem 5:92–98
- [5] Kausaite-Minkstimiene A, Kaminskas A, Gayda G, Ramanaviciene A (2024) Towards a self-powered amperometric glucose biosensor based on a single-enzyme biofuel cell. Biosensors 14:138. https://doi.org/10.3390/bios14030138
- [6] Li L, Zhou Y, Sun C, Zhou Z, Zhang J, Xu Y, Xiao X, Deng H, Zhong Y, Li G, Chen Z, Deng W, Hu X, Wang Y (2024) Fully integrated wearable microneedle biosensing platform for wide-range and real-time continuous glucose monitoring. Acta Biomater 175:199–213
- [7] Ma X, Zhang T, Wang X, Zhang T, Zhang R, Xu Z, Shi F (2023) Nanoparticles based on prussian blue for

- biosensor applications: a review. ACS Appl Nano Mater 6(24):22568-22593
- [8] Sheng J, Wu Y, Ding H, Feng K, Shen Y, Zhang Y, Gu N (2024) Multienzyme-like Nanozymes: regulation, rational design, and application. Adv Mater 36:2211210
- [9] Liu X, Xu H, Peng H, Wan L, Di D, Qin Z, He L, Lu J, Wang S, Zhao Q (2024) Advances in antioxidant nanozymes for biomedical applications. Coord Chem Rev 502:215610
- [10] Zeng H, Xie Y, Liu T, Chu Z, Dempsey E, Jin W (2024) Conductive polymer nanocomposites: recent advances in the construction of electrochemical biosensors. Sens Diagn 3:165
- [11] He H, Long M, Duana Y, Gu N (2023) Prussian blue nanozymes: progress, challenges, and opportunities. Nanoscale 15:12818
- [12] Matias TA, de Faria LV, Rocha RG, Silva MNT, Nossol E, Richter EM, Muñoz RAA (2022) Prussian blue-modified laser-induced graphene platforms for detection of hydrogen peroxide. Microchim Acta 189:188
- [13] Ramanaviciusa A, Inese Rekertaitea A, Valiunasa R, Valiuniene A (2017) Single-step procedure for the modification of graphite electrode by composite layer based on polypyrrole Prussian blue and glucose oxidase. Sens Actuators B 240:220–223
- [14] Cai Y, Liang B, Chen S, Zhu Q, Tu T, Wu K, Cao Q, Fang L, Liang X, Ye X (2020) a One-step modification of nanopolyaniline/glucose oxidase on double-side printed flexible electrode for continuous glucose monitoring: characterization, cytotoxicity evaluation and in vivo experiment. Biosens Bioelectron 165:112408
- [15] Komkova MA, Karyakina EE, Karyakin AA (2018) Catalytically synthesized Prussian Blue nanoparticles defeating natural enzyme peroxidase. J Am Chem Soc 140:11302-11307
- [16] Karyakin AA (2001) Prussian Blue and its analogues: electrochemistry and analytical applications. Electroanalysis 13:813–819
- [17] Komkova MA, Ibragimova OA, Karyakina EE, Karyakin AA (2021) Catalytic pathway of nanozyme "artificial peroxidase" with 100-fold greater bimolecular rate constants compared to those of the enzyme. J Phys Chem Letters 12:171–176
- [18] Fiorito PA, Gonçales VR, Ponzio EA, Torresi SIC (2005) Synthesis, characterization and immobilization of Prussian blue nanoparticles. A potential tool for biosensing devices. Chem. Commun. 3:366–368
- [19] Zhou PH, Xue DS, Luo HQ, Chen XG (2002) Fabrication, structure, and magnetic properties of highly ordered Prussian blue nanowire arrays. Nano Lett 2:845–847



- [20] Johansson A, Widenkvist E, Lu J, Boman M, Jansson U (2005) Fabrication of high aspect-ratio Prussian blue nanotubes using a porous alumina template. Nano Lett 5:1603–1606
- [21] Karyakin AA, Puganova EA, Budashov IA, Kurochkin IN, Karyakina EE, Levchenko VA, Matveyenko VN, Varfolomeyev SD (2004) Prussian Blue based nanoelectrode arrays for H2O2 detection. Anal Chem 76:474–478
- [22] Karyakin AA, Karyakina EE, Gorton L (1999) On the mechanism of H2O2 reduction at Prussian Blue modified electrodes. Electrochem Commun 1:78–82
- [23] Garjonyté R, Malinauskas A (1998) Electrocatalytic reactions of hydrogen peroxide at carbon paste electrodes modified by some metal hexacyanoferrates. Sens. Actuators. B 46:236–241
- [24] Niamsi W, Larpant N, Kalambate PK, Primpray V, Karuwan C (2022) Nadnudda rodthongkum 4,5 and wanida laiwattanapaisal 2paper-based screen-printed ionic-liquid/ graphene electrode integrated with prussian blue/mxene nanocomposites enabled electrochemical detection for glucose sensing. Biosensors 12:852
- [25] Karyakin AA, Karyakina EE (1999) Prussian Blue-based 'artificial peroxidase' as a transducer for hydrogen peroxide detection. Appl biosens, Sens Actuators B 57:268–273
- [26] Rojas D, Della Pelle F, Del Carlo M, d'Angelo M, Dominguez-Benot R, Cimini A, Escarp A, Compagnone D (2018) Electrodeposited Prussian Blue on carbon black modified disposable electrodes for direct enzyme-free H2O2 sensing in a Parkinson's disease in vitro model, sensors & actuators: b. Chemical 275:402–408
- [27] Barber R, Davis J, Papakonstantinou P (2023) Stable chitosan and prussian blue-coated laser-induced graphene skin sensor for the electrochemical detection of hydrogen peroxide in sweat. ACS Appl Nano Mater 6:10290–10302
- [28] Peng Z, Li Z, Liao J, Zhang Z, Song Y, Xia C, Xia Y, Wang Z (2024) Study of electrochemical biosensor for determination of glucose based on Prussian blue/gold nanoparticleschitosan nanocomposite film sensing interface Meas. Sci Technol 35:015125
- [29] Huang W, Guo P, Li B, Fu L, Lin C-T, Yu A, Lai G (2022) Enzyme-catalyzed deposition of polydopamine for amplifying the signal inhibition to a novel Prussian blue-nanocomposite and ultrasensitive electrochemical immunosensing. J Mater Sci Technol 102:166–173
- [30] Amarnath CA, Sawant SN (2019) Tailoring synthesis strategies for polyaniline-prussian blue composite in view of energy storage and H2O2 sensing application. Electrochim Acta 295:294–301

- [31] Cao Y, Shi H, Zheng Y, Tan Z, Xie Z, Zhang C, Chen Z (2023) H2O2 in EBC using an integrated condensation facemask. Sens Actuators, B Chem 393:134189
- [32] Shan Y, Han Y, Yao X, Liu T, Liu Y, Chu Z, Jin W (2023) A novel Prussian blue/PANI nanostructure-based biosensor for ultrasensitive determination of trace hydroquinone sensors & actuators: B. Chemical 393:134137
- [33] Uzunçar S, Ozdogan N, AkAn M (2021) Innovative sensor construction strategy via LbL Assembly for the detection of H2O2 based on the sequential in situ growth of Prussian Blue nanoparticles in CMC-PANI composite film. J Electrochem Soc 168:076509
- [34] Zheng Y, Wang H, Ma Z (2017) A nanocomposite containing Prussian Blue, platinum nanoparticles and polyaniline for multi-amplification of the signal of voltammetric immunosensors: highly sensitive detection of carcinoma antigen 125. Microchim Acta 184:4269–4277
- [35] Zare EN, Makvandi P, Ashtari B, Rossi F, Motahari A, Perale G (2020) Progress in conductive polyaniline-based nanocomposites for biomedical applications: a review. J Med Chem 63:1–22
- [36] Sen T, Mishra S, Shimpi NG (2016) Synthesis and sensing applications of polyaniline nanocomposites: a review. RSC Adv 6:42196
- [37] Babel V, Hiran BL (2021) A review on polyaniline composites: Synthesis, characterization, and applications. Polym Compos 42:3142–3157
- [38] Liao G, Li Q, Xu Z (2019) The chemical modification of polyaniline with enhanced properties: a review. Prog Org Coat 126:35–43
- [39] Dash MP, Tripathy M, Sasmal A, Mohanty GC, Nayak PL (2010) Poly(anthranilic acid)/multi-walled carbon nanotube composites: spectral, morphological, and electrical properties. J Mater Sci 45:3858–3865
- [40] Benyoucef A, Huerta F, Vazquez JL, Morallon E (2005) Synthesis and in situ FTIRS characterization of conducting polymers obtained from aminobenzoic acid isomers at platinum electrodes. Eur Polymer J 41:843–852
- [41] Al-Hossainy AF, Bassyouni M, Zoromba MS (2018) Elucidation of electrical and optical parameters of poly(o-anthranilic acid)-poly(o-amino phenol)/copper oxide nanocomposites thin films. J Inorg Organomet Polym Mater 28:2572–2583
- [42] Metwally AM, Shaaban AF, Azab MM, Mahmoud AA, Ali HM (2020) Synthesis, characterization, morphology and adsorption performance towards Cu+2 ions of nanosized copolymers of anthranilic acid and o-aminophenol poly(anthranilic acid-co-o-aminophenol). J Polym Res 27:90



- [43] Chao D, Lu X, Chen J, Zhang W, Wei Y (2006) Anthranilic acid assisted preparation of Fe3O4-poly(aniline-coo-anthranilic acid) nanoparticles. J Appl Polym Sci 102:1666-1671
- [44] Mohammed Hosny N, Nowesser N, Al-Hussaini AS, Zoromba MS (2016) Doped copolymer of polyanthranilic acid and o-aminophenol (AA-co-OAP): Synthesis, spectral characterization and the use of the doped copolymer as precursor of a-Fe2O3 nanoparticles. J Mol Struct. 1106:479–484
- [45] Hosny NM, Al-Hussaini AS, Nowesser N, Zoromba MS (2016) Polyanthranilic acid Effect of inclusion of some transition metal ions and use of the doped polymer in synthesizing a-Fe2O3 nanoparticles via thermal decomposition rout. J Therm Anal Calorim. 124:287–293
- [46] Amaya T, Abe Y, Inada Y, Hirao T (2014) Synthesis of self-doped conducting polyaniline bearing phosphonic acid. Tetrahedron Lett 55:3976–3978
- [47] Khan M, Answer T, Mohammad F (2018) Sulphonated polyaniline/MWCNTs nanocomposite: preparation and promising thermoelectric performance, International. Nano Lett 8:213–220
- [48] Shojaei J, Zanganeh AR (2020) Electrochemically imprinted self-doped polyaniline as highly sensitive voltammetric sensor for determination of bismuth in water, wastewater, and pharmaceutical samples. J Mater Sci: Mater Electron 31:7182-7192
- [49] Casimero C, Hegarty C, McGlynn RJ, Davis J (2020) Ultrasonic exfoliation of carbon fiber: electroanalytical perspectives. J Appl Electrochem 50:383–394
- [50] Jerez-Masaquiza MD, Fernández L, González G, Montero-Jiménez M, Espinoza-Montero PJ (2020) Electrochemical sensor based on prussian blue electrochemically deposited at zro2 doped carbon nanotubes glassy carbon modified electrode. Nanomaterials 10(7):1328. https://doi.org/10. 3390/nano10071328
- [51] Liu J, Tian Y, Chen Y, Liu J, Tian Y, Chen Y, Liang J, Zhang L, Fong H (2010) A surface treatment technique of electrochemical oxidation to simultaneously improve the interfacial bonding strength and the tensile strength of PAN based carbon fibers. Mater Chem Phys 122:548–555
- [52] Zhang G, Sun S, Yang D, Zhang G, Sun S, Yang D, Dodelet J-P, Sacher E (2008) The surface analytical characterization of carbon fibers functionalized by H2SO4/ HNO3 treatment. Carbon 46:196–205
- [53] Z. Gao, J. Zhu, S. Rajabpour, K. Joshi, M. Kowalik, B. Croom, Y. Schwab, L. Zhang, C. Bumgardner, K.R. Brown, D. Burden, J.W. Klett, A.C.T. van Duin, L.V. Zhigilei, X. Li, Graphene Reinforced Carbon Fibers. Sci. Adv. 6 (2020) No. eaaz4191

- [54] F. Rosenburg, E. Ionescu, N. Nicoloso, R. Riedel, High-Temperature Raman Spectroscopy of Nano-Crystalline Carbon in Silicon Oxycarbide. Materials 11 (2018) No. 93
- [55] Moretti G, Gervais C (2018) Raman spectroscopy of the photosensitive pigment Prussian blue. J Raman Spectrosc 49:1198–1204
- [56] Nappini S, Matruglio A, Naumenko D, Zilio SD, Lazzarino M, De Groot FMF, Kocabas C, Balci O, Magnano E (2017) Graphene nanoreactors: photoreduction of prussian blue in aqueous solution. J Phys Chem C 121:22225–22233
- [57] Barsan MM, Butler IS, Fitzpatrick J, Gilson DFR (2011) High-pressure studies of the micro-raman spectra of iron cyanide complexes: prussian blue (Fe4[Fe(CN)6]3), potassium ferricyanide (K3[Fe(CN)6]), and sodium nitroprusside (Na2[Fe(CN)5(NO)]· 2H2O). J Raman Spectrosc 42:1820–1824
- [58] Qin M, Ren W, Meng J, Wang X, Yao X, Ke Y, Li Q, Mai L (2019) Realizing superior Prussian Blue positive electrode for potassium storage via ultrathin nanosheet assembly. ACS Sustain Chem Eng 7:11564–11570
- [59] You Y, Wu X-L, Yin Y-X, Guo Y-G (2014) High-quality Prussian Blue crystals as superior cathode materials for room-temperature sodium-ion batteries. Energy Environ Sci 7:1643–1647
- [60] Ji X, Ren J, Ni R, Liu X (2010) blue layer electrodeposited on self-assembled monolayers for constructing highly sensitive glucose biosensor. Analyst 135:2092
- [61] De Mattos IL, Gorton L, Ruzgas T, Karyakin AA (2000) Sensor for hydrogen peroxide based on prussian blue modified electrode: improvement of the operational stability. Anal Sci 16:795–798
- [62] Al-Hussaini AS, Zoromba MS, El-Ghamaz NA (2013) In situ polymerization and characterization of aniline and o-anthranilic acid copolymer/pyrogenic silica nanocomposites. Polym-Plast Technol Eng 52:1089–1096
- [63] Nikitina VN, Zavolskova MD, Karyakin AA (2023) Protein-sized nanozymes «artificial peroxidase» based on template catalytic synthesis of Prussian Blue. Bioelectrochemistry 149:108275
- [64] Berkkan A, Seçkin AI, Pekmez K, Tamer U (2010) Amperometric enzyme electrode for glucose determination based on poly(pyrrole-2-aminobenzoic acid). J Solid State Electrochem 14:975–980

Publisher's Note Springer Nature remains neutral with regard to jurisdictional claims in published maps and institutional affiliations.

